physical sciences forum

MDPI

Proceeding Paper

Sensitivity to Cabibbo-Suppressed Λ Production in MicroBooNE †

Christopher Thorpe on behalf of the MicroBooNE Collaboration

Physics Department, Lancaster University, Lancaster LA1 4YW, UK; c.thorpe@lancaster.ac.uk

† Presented at the 23rd International Workshop on Neutrinos from Accelerators, Salt Lake City, UT, USA, 30–31 July 2022.

Abstract: The MicroBooNE detector is a liquid argon time projection chamber (LArTPC) with an 85 ton active mass that receives flux from the Booster Neutrino and the Nutrinos from the Main Injector (NuMI) beams, providing excellent spatial resolution of the reconstructed final-state particles. Since 2015, MicroBooNE has accumulated many neutrino and anti-neutrino scattering events with argon nuclei enabling searches for rare interaction channels. The Cabibbo-suppressed production of hyperons in anti-neutrino–nucleus interactions provides sensitivity to a range of effects, including second-class currents, SU(3) symmetry violations and reinteractions between the hyperon and the nuclear remnant. This channel exclusively involves anti-neutrinos, offering an unambiguous constraint on wrong-sign contamination. The effects of nucleon structure and final state interactions are distinct from those affecting the quasielastic channel and modify the Λ and Σ production cross sections in different ways, providing new information that could help to break their degeneracy. Few measurements of this channel have been made, primarily in older experiments such as Gargamelle. We present the sensitivity of the MicroBooNE experiment to the cross section for direct (Cabibbo-suppressed) Λ production in muon anti-neutrino interactions, using anti-neutrinos from the off-axis NuMI beam.

Keywords: neutrino interactions; hyperons; LArTPC

Citation: Thorpe, C., on behalf of the MicroBooNE Collaboration. Sensitivity to Cabibbo-Suppressed Λ Production in MicroBooNE. *Phys. Sci. Forum* **2023**, *8*, 16. https://doi.org/10.3390/psf2023008016

Academic Editor: Yue Zhao

Published: 20 July 2023

1. Introduction

The Cabibbo-suppressed production of hyperons is a rare neutrino interaction process with few measurements [1–6], subject to unique nuclear effects such as hyperon-nucleus potentials which modify the cross sections of the individual channels in different ways. This creates potential to disentangle the physics of the initial anti-neutrino–nucleon interaction from final-state interactions [7]. This paper presents the sensitivity of the MicroBooNE experiment [8] to the cross section of Cabibbo-suppressed Λ production:

$$\bar{\nu}_\mu + \mathrm{Ar} \rightarrow \mu^+ + \Lambda + X. \tag{1}$$

This calculation assumes data corresponding to 2.2×10^{20} protons on target (POT) of neutrino mode flux and 4.9×10^{20} POT of anti-neutrino mode flux from the Neutrinos from the Main Injector (NuMI) beam [9,10], which will be analyzed. The data from these periods are combined to minimize the statistical uncertainty in the measurement.

2. Event Selection

Neutrino interactions are reconstructed using the Pandora [11] reconstruction/pattern recognition framework, which identifies a candidate neutrino interaction vertex and reconstructs the resulting tracks and electromagnetic showers. These objects are analyzed by event selection, which applies a set of criteria to reject background interactions. Prior to applying any event selection, 37 signal events are predicted, among a background of

1.6 million events. The background comprises other neutrino interactions and cosmic rays mistakenly tagged as particles resulting from neutrino interactions.

Any events in which the reconstructed vertex is outside of the fiducial volume used in Ref. [12] are rejected. The selection searches for the $\Lambda \to p + \pi^-$ decay, which creates a V-shaped signature in the detector, seen in Figure 1. There are three final-state particles that must be identified: the μ^+, p and π^-, all of which produce track-like signatures. Any events containing fewer than three reconstructed tracks or any showers are rejected. Particle identification (PID) scores [13] are employed to analyze the calorimetric information associated with these tracks, indicating if they are muon-like or proton-like. The longest muon-like track is the muon candidate. A pair of tracks consistent with a proton and charged pion are identified using an array of boosted decision trees [14], leveraging variables such as PID scores [13] and Pandora's track/shower classification score [15]. From this pair of tracks, two kinematic quantities are calculated: their invariant mass, displayed in Figure 2a, and angular deviation, denoted as α in Figure 2b. The angular deviation is defined as the angle between the reconstructed momentum vector of the Λ candidate and the line joining the primary vertex to the decay vertex. Cuts are applied to these variables to remove events with kinematics inconsistent with a decaying Λ baryon. Finally, the "island finding" method, illustrated in Figure 3, is employed to determine whether the proton and pion form a true displaced vertex.

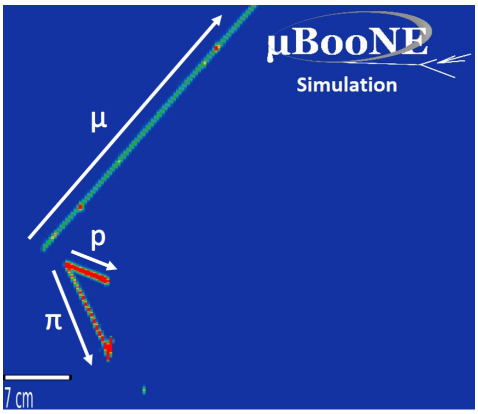

Figure 1. Event display of simulated signal event. The different colors indicate ionization of the argon in the detector, with green/red indicating weaker/stronger ionization.

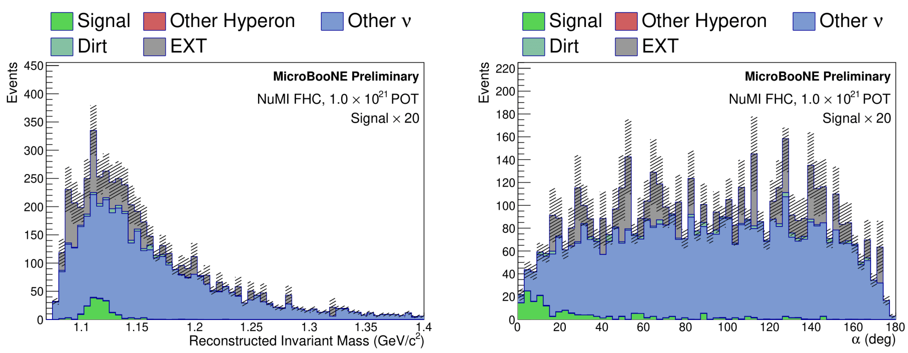

(**a**) Reconstructed invariant mass. (**b**) Angular deviation.

Figure 2. Kinematic variables employed by the selection, with the signal strength multiplied by 20 for visibility. Events with 1.09 < reconstructed invariant mas < 1.14 GeV/c and $\alpha < 14^\circ$ are selected.

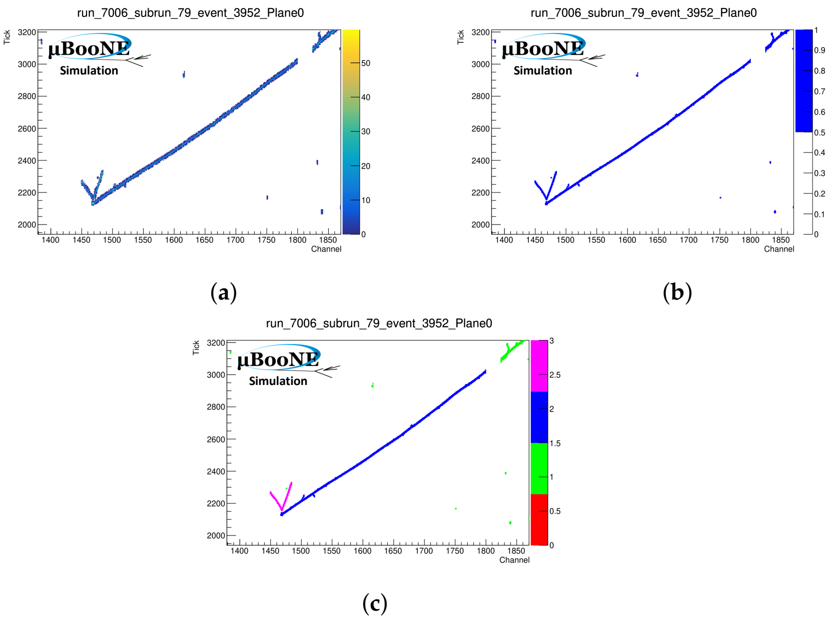

Figure 3. Three stages of the island finding, applied to a signal MC simulation event. The deconvolved wire activity is filtered, removing any pixels below a threshold value. The starting positions of the tracks, mapped into wire-time space coordinates, are used to determine if the proton and pion form a separate island to the muon. (**a**) Deconvolved wire signals. (**b**) After application of the threshold filter. (**c**) After generating islands. The blue region is the muon island, the pink the combined proton/pion island. Green represents unused activity.

After applying the selection, the surviving events consist of the signal, other events in which Λ baryons are produced (such as deep inelastic scattering or resonance excitation), other hyperons such as the Σ^0, events containing secondary interactions of neutrons and events containing reconstruction problems. The efficiency of the event selection is 7% with a final purity of 47%, suppressing the background by a factor of $\sim 10^6$.

3. Systematic Uncertainties

Four sources of systematic uncertainties are considered: the neutrino flux [16], cross sections of background neutrino interaction processes [17], cross sections of secondary interactions simulated by GEANT 4 [18,19] and the detector response [20]. The dominant source of uncertainty in the predicted signal is the flux.

4. Cross-Section Extraction

The cross-section extraction procedure involves generating pseudo-experiments and repeatedly calculating the cross section in each to estimate the effect of uncertainties, including the asymmetric shapes of the statistical uncertainties. To propagate the MC simulation statistical uncertainties, the Bayesian posterior distributions of the selection efficiency ϵ, and the selected background, B, are calculated with uniform priors using the TEfficiency class [21]. The data's statistical uncertainty is modeled by applying Bayes' theorem to the Poisson distribution, yielding the posterior distribution $P(N|N_{\mathrm{obs}})$ when N_{obs} events are observed in the data.

The systematic uncertainties are propagated by first calculating the covariance matrix of the selection efficiency ϵ, the total muon anti-neutrino flux Φ, and the selected background B and constructing a three-dimensional Gaussian distribution, from which systematic fluctuations $\alpha_\epsilon, \alpha_\Phi$ and α_B may be sampled. Pseudo-experiments are then generated by sampling values of $\epsilon, B, N, \alpha_\epsilon, \alpha_\Phi$ and α_B from their respective distributions and calculating their resulting cross section with

$$\sigma_* = \frac{N - (B + \alpha_B)}{T(\Phi + \alpha_\Phi)\Gamma(\epsilon + \alpha_\epsilon)}. \tag{2}$$

The resulting distributions are drawn, for N_{obs} ranging from 0 to 7, in Figure 4, compared with the cross section predicted by MicroBooNE's GENIE tune [17].

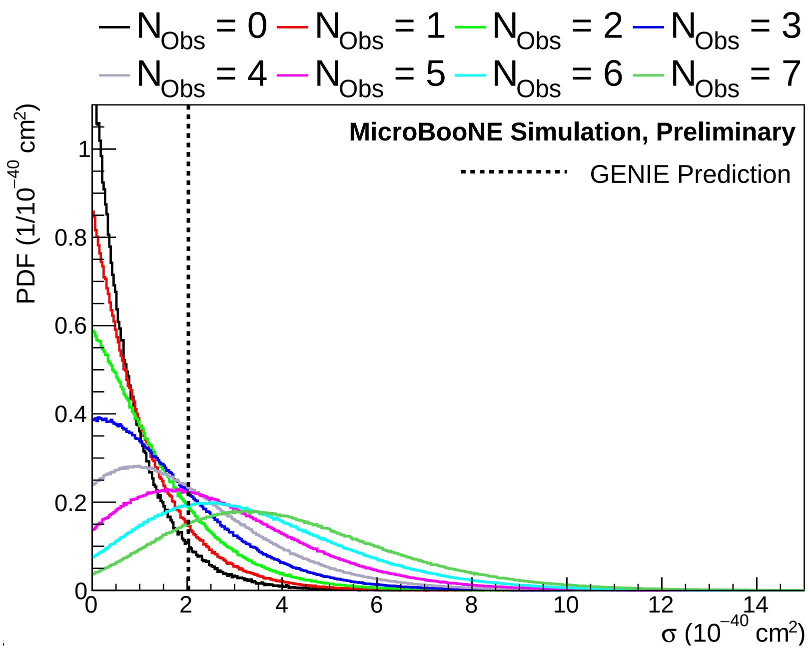

Figure 4. Bayesian posterior probability distributions of the cross section for different values of N_{obs}, compared with the value predicted by MicroBooNE's GENIE tune [17].

5. Summary

A complete procedure for the extraction of the cross section of the Cabibbo-suppressed production of Λ baryons has been developed, and is ready for application to MicroBooNE data. A sophisticated event selection is employed, reducing an initial background of 1.6 million events to $\sim$3 events, against a predicted signal of 2.5 events. The final sensitivity is expressed as a collection of Bayesian posterior probability distributions, calculated by generating pseudo-experiments in which the quantities used to calculate the cross section are varied according to their uncertainties.

Funding: This document was prepared by the MicroBooNE collaboration using the resources of the Fermi National Accelerator Laboratory (Fermilab), a U.S. Department of Energy, Office of Science, HEP User Facility. Fermilab is managed by Fermi Research Alliance, LLC (FRA), acting under Contract No. DE-AC02-07CH11359. MicroBooNE is supported by the following: the U.S. Department of Energy, Office of Science, Offices of High Energy Physics and Nuclear Physics; the U.S. National Science Foundation; the Swiss National Science Foundation; the Science and Technology Facilities Council (STFC), part of the United Kingdom Research and Innovation; the Royal Society (United Kingdom); and the UK Research and Innovation (UKRI) Future Leaders Fellowship. Additional support for the laser calibration system and cosmic ray tagger was provided by the Albert Einstein Center for Fundamental Physics, Bern, Switzerland. We also acknowledge the contributions of technical and scientific staff to the design, construction, and operation of the MicroBooNE detector as well as the contributions of past collaborators to the development of MicroBooNE analyses, without whom this work would not have been possible. For the purpose of open access, the authors have applied a Creative Commons Attribution (CC BY) public copyright license to any Author Accepted Manuscript version arising from this submission.

Institutional Review Board Statement: Not applicable.

Informed Consent Statement: Not applicable.

Data Availability Statement: Not applicable.

Conflicts of Interest: The author declares no conflict of interest.

References

1. Ammosov, V.V.; Denisov, A.G.; Gapienko, G.S.; Gapienko, V.A.; Klyukhin, V.I.; Koreshev, V.I.; Pitukhin, P.V.; Sirotenko, V.I.; Usubov, Z.U.; Zaetz, V.G.; et al. Neutral Strange Particle Exclusive Production in Charged Current High-energy Anti-neutrino Interactions. *Z. Phys. C* **1987**, *36*, 377–381. [CrossRef]
2. Eichten, T.; Faissner, H.; Kabe, S.; Frenz, W.; Krogh, J.V.; Morfin, J.; Schultze, K.; Lemonne, J.; Sacton, J.; Donnick, W.V.; et al. Observation of 'Elastic' Hyperon Production by Anti-neutrinos. *Phys. Lett.* **1972**, *40*, 593–596. [CrossRef]
3. Erriquez, O.; Muciaccia, M.T.F.; Natali, S.; Nuzzo, S.; Halsteinslid, A.; Jarlskog, C.; Myklebost, K.; Rognebakke, A.; Skjeggestad, O.; Tvedt, B.; et al. Production of Strange Particles in Anti-neutrino Interactions at the CERN PS. *Nucl. Phys. B* **1978**, *140*, 123–140. [CrossRef]
4. Erriquez, O.; Muciaccia, M.T.F.; Natali, S.; Nuzzo, S.; Halsteinslid, A.; Myklebost, K.; Rognebakke, A.; Skjeggestad, O.; Bonetti, S.; Cavalli, D.; et al. Strange Particle Production by Antineutrinos. *Phys. Lett. B* **1977**, *70* 383–386. [CrossRef]
5. SKAT; Brunner, J.; Grabosch, H.-J.; Kaufmann, H.H.; Nahnhauer, R.; Nowak, S.; Schlenstedt, S.; Ammosov, V.V.; Ermolaev, V.I.; Ivanilov, A.A.; et al. Quasielastic Nucleon and Hyperon Production by Neutrinos and Anti-neutrinos with Energies Below 30 GeV. *Z. Phys. C* **1990**, *45*, 551–555. [CrossRef]
6. Fanourakis, G.; Resvanis, L.K.; Grammatikakis, G.; Tsilimigras, P.; Vayaki, A.; Camerini, U.; Fry, W.F.; Loveless, R.J.; Mapp, J.H.; Reeder, D.D. Study of Low-Energy Antineutrino Interactions on Protons. *Phys. Rev. D* **1980**, *21*, 562. [CrossRef]
7. Thorpe, C.; Nowak, J.; Niewczas, K.; Sobczyk, J.T.; Juszczak, C. Second Class Currents, Axial Mass, and Nuclear Effects in Hyperon Production. *Phys. Rev. C* **2021**, *104*, 035502. [CrossRef]
8. MicroBooNE Collaboration; Acciarri, R.; Adams, C.; An, R.; Aparicio, A.; Aponte, S.; Asaadi, J.; Auger, M.; Ayoub, N.; Bagby, L.; et al. Design and Construction of the MicroBooNE detector. *J. Instrum.* **2017**, *12*, P02017. [CrossRef]
9. MINERvA Collaboration; Aliaga, L.; Kordosky, M.; Golan, T.; Altinok, O.; Bellantoni, L.; Bercellie, A.; Betancourt, M.; Bravar, A.; Budd, H.; et al. Neutrino Flux Predictions for the NuMI Beam. *Phys. Rev. D* **2016**, *94*, 092005. [CrossRef]
10. Adamson, P.; Anderson, K.; Andrews, M.; Andrews, R.; Anghel, I.; Augustine, D.; Aurisano, A.; Avvakumov, S.; Ayres, D.S.; Baller, B.; et al. The NuMI Neutrino Beam. *Nucl. Instrum. Meth. A* **2016**, *806*, 279–306. [CrossRef]
11. MicroBooNE Collaboration; Acciarri, R.; Adams, C.; An, R.; Anthony, J.; Asaadi, J.; Auger, M.; Bagby, L.; Balasubramanian, S.; Baller, B.; et al. The Pandora Multi-algorithm Approach to Automated Pattern Recognition of Cosmic-ray Muon and Neutrino Events in the MicroBooNE Detector. *Eur. Phys. J. C* **2018**, *78*, 82. [CrossRef] [PubMed]
12. MicroBooNE Collaboration; Abratenko, P.; Alrashed, M.; An, R.; Anthony, J.; Asaadi, J.; Ashkenazi, A.; Balasubramanian, S.; Baller, B.; Barnes, C.; et al. Cosmic Ray Background Rejection with Wire-Cell LArTPC Event Reconstruction in the MicroBooNE Detector. *Phys. Rev. Appl.* **2021**, *15*, 064071. [CrossRef]
13. MicroBooNE Collaboration; Abratenko, P.; An, R.; Anthony, J.; Asaadi, J.; Ashkenazi, A.; Balasubramanian, S.; Baller, B.; Barnes, C.; Barr, G.; et al. Calorimetric Classification of Track-like Signatures in Liquid Argon TPCs using MicroBooNE Data. *J. High Energy Phys.* **2021**, *12*, 153. [CrossRef]
14. Hoecker, A.; Speckmayer, P.; Stelzer, J.; Therhaag, J.; von Toerne, E.; Voss, H.; Backes, M.; Carli, T.; Cohen, O.; Christov, A. et al. TMVA—Toolkit for Multivariate Data Analysis. *arXiv* **2007**, arXiv:physics/0703039.
15. Van De Pontseele, W. Search for Electron Neutrino Anomalies with the MicroBooNE Detector. Ph.D. Thesis, University of Oxford, Oxford, UK, 2020.
16. Aliaga Soplin, L. Neutrino Flux Prediction for the NuMI Beamline. Ph.D. Thesis, College of William and Mary, Williamsburg, VA, USA, 2016.
17. MicroBooNE Collaboration; Abratenko, P.; An, R.; Anthony, J.; Arellano, L.; Asaadi, J.; Ashkenazi, A.; Balasubramanian, S.; Baller, B.; Barnes, C.; et al. New CC0π GENIE Model Tune for MicroBooNE. *Phys. Rev. D* **2022**, *105*, 072001. [CrossRef]
18. GEANT4; Agostinelli, S.; Allison, J.; Amako, K.; Apostolakis, J.; Araujo, H.; Arce, P.; Asai, M.; Axen, D.; Banerjee, S.; et al. GEANT 4–A Simulation Toolkit. *Nucl. Instrum. Meth. A* **2003**, *506*, 250–303. [CrossRef]
19. Calcutt, J.; Thorpe, C.; Mahn, K.; Fields, L. Geant4Reweight: A Framework for Evaluating and Propagating Hadronic Interaction Uncertainties in Geant4. *J. Instrum.* **2021**, *16*, P08042. [CrossRef]

20. MicroBooNE Collaboration; Abratenko, P.; An, R.; Anthony, J.; Arellano, L.; Asaadi, J.; Ashkenazi, A.; Balasubramanian, S.; Baller, B.; Barnes, C.; et al. Novel Approach for Evaluating Detector-Related Uncertainties in a LArTPC Using MicroBooNE Data. *Eur. Phys. J. C* **2022**, *82*, 454. [CrossRef]
21. Root Version 6.16 Used. Available online: https://root.cern.ch/doc/master/classTEfficiency.html (accessed on 21 November 2023).